Analysis of the influencing factors on the tribological properties of peanut straw

Xiaoyu Wang[1], Guoming Li[2], Xin He[3], Rusha Yang[4], Qiangji Peng[1], Chunyan Zhang[1], Ningning Zhang[1], Jianming Kang[1*]

(1. *Shandong Academy of Agricultural Machinery Science, Jinan 250100, China*;
2. *College of Agricultural Engineering and Food Science, Shandong University of Technology, Zibo 255100, Shandong, China*;
3. *School of Mechanical and Automotive Engineering, Liaocheng University, Liaocheng 252000, Shandong, China*;
4. *Shandong Department of Agriculture and Rural Affairs, Jinan 250013, China*)

Abstract: Chopped straws can help replenish soil nutrients, improve soil structure, and increase the amount of organic matter contained in soil. The grinding ability of crop straws is influenced by the frictional characteristics of the materials involved in the grinding process. Studying the frictional properties of peanut stem, residual film, and external contact material is essential to understanding the grinding action of peanuts. This study discussed the frictional properties between films and between residual film and external contact materials. A physical test was conducted using a friction coefficient detector. The results showed that the average value of the dynamic sliding friction coefficient (f_k) was 0.34, the average value of the static sliding friction coefficient (f_s) between the film and the 40Cr steel plate (as the external contact material) was 0.38, and the average f_s value between the films and between the residual film and the external contact material was 0.36. Based on the Box-Behnken test, second-order response models were established for the static rolling stability angle (μ_e) and the static sliding friction coefficient (f_s). On the basis of establishing the static rolling stability angle (μ_e) and static sliding friction coefficient (f_s) of the evaluation index, the different friction characteristics between straw and external contact materials were investigated under varying moisture content, external contact materials and particle sizes. The study results can provide a basis for the development of equipment that can be used for peanut straw crushing and membrane separation.

Keywords: peanut straw, residual film, friction characteristics
DOI: 10.25165/j.ijabe.20241706.9114

Citation: Wang X Y, Li G M, He X, Yang R S, Peng Q J, Zhang C Y, et al. Analysis of the influencing factors on the tribological properties of peanut straw. Int J Agric & Biol Eng, 2024; 17(6): 76–85.

1 Introduction

Peanut film cultivation is an efficient planting technology for increasing yield and income, with advantages such as heat and water preservation, grass suppression and seedling promotion, and improved satiation rate[1]. In recent years, peanut film mulching has become increasingly common in North China and Northeast China. Although the yield per unit area of peanuts has improved to a certain extent, it is difficult to recover the residual mulching film. Currently, the mechanized residual film contains a large number of granular substances, such as soil, and impurities such as peanut straws[2], and the physical properties and structural characteristics of the residual film and peanut straws are significantly different. It is difficult to separate membrane impurities, which increases the utilization cost of peanut straws due to their contact and entanglement. As a pre-treatment link for crop straw cleaning and secondary utilization, crushing is an effective means to improve the separation efficiency of membrane impurities, and it is of great significance in improving the recycling level of straw resources and farmers' economic benefits. Hence, for effective utilization of peanut straws, the membrane mixture should be effectively chopped after harvest[3-5]. The shape and scale of the residual film and peanut straws can be reduced, and the degree of entanglement between the residual film and peanut straw can be reduced, providing a prerequisite for the efficient separation of the residual film, straw, and soil, and a high-quality recovery of the residual film and peanut straws.

The physical characteristic parameters of agricultural materials, such as peanut straws and residual films, are important engineering data that can be utilized in the design and development of agricultural machinery and agricultural product processing machinery, and they also serve as basic theoretical support[6-9]. The friction between the materials in a film mixture and the friction between the material and the external contact material affects the mechanical behavior of materials[10-12]. Moreover, a rubbing effect of the mixture is simultaneously generated by the friction between the materials, thereby facilitating the enhancement of its shredding effect. This phenomenon holds significant implications for investigating the separation process of mixtures.

Based on this background, an investigation into the friction characteristics between peanut stalks, and between peanut stalks and

Received date: 2024-06-04 **Accepted date:** 2024-11-11
Biographies: Xiaoyu Wang, MS, research interest: agricultural machinery and equipment, Email: wangxiaoyusdut@163.com; **Guoming Li**, MS, research interest: agricultural machinery and equipment, Email: 1466719941@qq.com; **Xin He**, MS, research interest: Intelligent agricultural machinery, Email: 3054505842@qq.com; **Rusha Yang**, Title BS, research interest: extension of agricultural mechanization technology, Email: 1470179542@qq.com; **Qiangji Peng**, PhD, research interest: agricultural machinery and equipment and intelligent control, Email: pengqiangji@shandong.cn; **Chunyan Zhang**, MS, research interest: agricultural machinery and equipment, Email: sdnjyzcy@163.com; **Ningning Zhang**, MS, research interest: agricultural machinery and equipment, Email: ning0716@126.com.
***Corresponding author: Jianming Kang**, PhD, research interest: agricultural machinery and equipment and key technologies. Shandong Academy of Agricultural Machinery Sciences, Jinan 250100, China. Tel: +86-15624389451, Email: kjm531@sina.com.

residual film, as well as their interaction with external contact materials to determine the frictional characteristic parameters, holds significant implications for studying the shredding mechanism of hybrid film mixtures and the design and development of related technical equipment[13,14]. Fang et al.[15] considered soybean straw as the test subject to study the sliding friction angle between soybean straw, steel plate, and rubber belt under different water content conditions, and performed experimental research. Sui et al.[16] considered maize straw as the research subject and analyzed the effects of different moisture contents, crushing sizes, and gaps between rollers on the straw extrusion molding process through a single-factor test. Shinners et al.[17] discussed the sliding friction coefficient of alfalfa straw in terms of moisture content, pressure, relative movement speed, and external contact materials. Li et al.[18] measured the sliding friction coefficient of ceramic particles and a maize straw mixture with different particle sizes along an inclined plane and an outer pipe through experiments. The sliding friction coefficient of the mixture was approximately linear with the theoretical volume coefficient of each component, and most of the apparent values were greater than the corresponding values of pure substances. Phani et al.[19] considered granular straws after the crushing of barley, rape, and oats as the research subjects; no treatment and steam blasting treatment were employed as the variables to study the laws of their influence on the friction coefficient of the straws. Yang et al.[20] studied the effects of moisture content, external contact material, shear rate, vertical stress, and other factors on the friction characteristics of millet. They found that the moisture content had no evident effect on the appearance of the millet, but it significantly affected its static sliding friction factor, and the friction coefficients between the two materials were also very different. Zhang et al.[21] measured the friction characteristics of Gorgon Euryale fruits with different maturity levels and particle sizes; the smaller the fruit particles, the greater the number of particles in contact with each other in a unit area, and the greater the mesh and inlay effect on the surface of each particle, resulting in a greater friction resistance. Lu et al.[22] established a trivariate regression equation based on the testing and simulation of the friction characteristics of rice bud species, solved the regression equation numerically, and obtained the main contact parameters that met the requirements. Lu et al.[23] conducted experiments on wheat and maize straws with different water contents, angles, contact locations, and external contact materials. They determined the separate and interactive effects of these factors on the tribological properties of the straws. Liang et al.[24,25] applied the response surface method to study the friction characteristics between cotton culm, residual film, and external contact materials; analyzed the contact states between cotton culms with different moisture contents and sampling locations; and investigated the friction characteristics between the residual film and external contact materials. The friction characteristics between the cotton culm, residual film, and external contact material were revealed by measuring the static and dynamic friction coefficients under different influencing factors. The static and dynamic friction coefficients of different types of residual films were measured, and the contact parameters between them and the residual films were determined. The EDEM analysis method was used to calibrate the recovery coefficient and static friction coefficient between the residual films.

In summary, scholars have studied the friction characteristics between residual films and different crop stalks and seeds, accumulating rich basic data for agricultural machinery design and simulation analysis. However, currently, research on the friction characteristics of peanut stalk residual film mixtures is in its infancy, and there is a lack of comparison and analysis of simulation data with actual data. Therefore, there is room to better understand the relevant mechanism and develop related equipment.

In view of the respective physical characteristics of peanut straws, residual film, and external contact materials, studying the frictional properties associated with the relative movement of these materials during the separation process is important. Hence, the objectives of this work are as follows:

1) The friction characteristics of the residual film and peanut straws were quantitatively characterized through a dynamic–static friction coefficient measuring instrument combined with a self-developed tilt measuring instrument. With this, the change laws of the dynamic and static friction coefficients of the residual film and peanut straws were determined.

2) Through orthogonal testing, the effects of the particle size, moisture content, and external contact material on the friction properties of several materials were investigated. Based on this, a mathematical relationship between the static rolling stability and static sliding friction coefficient was established. To reveal the mechanisms whereby diverse elements influence the frictional quality of the residue film-peanut straw, an angle was formed using rods under varying particle sizes, moisture contents, and external contact materials.

The results of this study were expected to build upon the theoretical foundation for the development of physical models of peanut straws, improve the consistency between the theoretical and experimental results, and contribute to the design of critical parts for the crushing of mixed membrane materials.

2 Test materials and methods

2.1 Test materials and instruments

The test was performed in January 2024, and the test site was the Key Laboratory of Huang Huaihai Peanut Production Area of the Agricultural and Rural Department of Shandong Academy of Agricultural Machinery Science. The test materials were taken from the peanut test field of the Shandong Academy of Agricultural Machinery in October 2023. The instruments used in the test were MXD-01-type static and dynamic friction coefficient detector (Jinan Languang Electromechanical Technology Co., Ltd., China; load range: 0-5 N, stroke: 10-60 mm); self-made bevel meter (angle adjustment range: 0°-70°); DHS-20A halogen rapid water meter (Shanghai Jinghai Instrument Co., Ltd., China; maximum weighing value: 110 g, water reading: 0.01%); JA51002 electronic balance (Shanghai Jinghai Instrument Co., Ltd. Weighing range: 0-5100 g, Reading accuracy: 0.01 g); DHG101-0-type electric blast drying oven (Shanghai Hetian Scientific Instrument Co., Ltd., China; Temperature control: 50°C-250°C, temperature resolution: 0.1°C, temperature fluctuation: ±1°C). In addition to the above equipment, test measuring tools and auxiliary tools included Vernier calipers, 40Cr steel plates (Correspondence standard: GB/T3077-2015, Alloy structure steels), residual film, scissors, wallpaper knives, etc.

2.2 Test methods and evaluation criteria

2.2.1 Procedure for testing the frictional properties between peanut straw and residual film

In the measurement of the dynamic and static friction coefficients between the residual films, an agricultural film from the same manufacturer was selected, and regions in the film with poor quality, such as the opening and edges, were avoided. Following the same texture direction, the residual film was cut into dimensions of

120 mm×100 mm and 200 mm×100 mm to measure the dynamic and static friction coefficients between the films. The residual film was then attached to the working horizontal surface of the tester and the bottom surface of the sliding block of the static friction coefficient tester. Finally, a (200+2) g pressing block was placed on the top surface of the sliding block (Figure 1). To ensure that there was no damage, bubbles, or folding and that the bottom surface of the slider was in perfect contact with the upper surface of the working level, the slider was moved at a speed of (100±10) mm/min by the national standard GB/T10006-2021. Ten groups of experiments were conducted, each group of tests was conducted thrice, and the arithmetic average was taken as the final result.

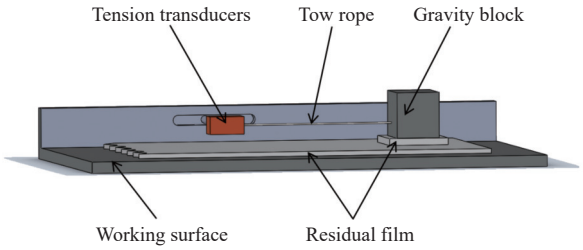

Figure 1 Test setup for measuring the dynamic and static friction coefficients between membranes and between films

Because the material of the cutting tool, roller, and other key parts in direct contact with the straw of the peanut straw crushing and separation machine is 40Cr, the external contact material selected in the test was 40Cr[26]. The 40Cr steel plate was made to adhere to the working surface of the bevel meter using a self-made bevel meter, and the pressure block wrapped in the residual film was placed on the upper surface of the 40Cr steel plate to measure the static sliding friction coefficient between the residual film and the 40Cr plate (Figure 2).

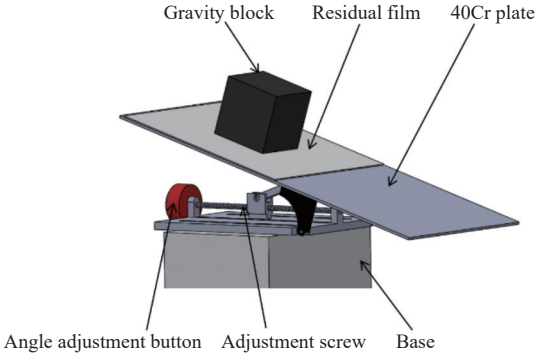

Figure 2 Setup of the static sliding friction coefficient test between residual film and 40Cr steel plate

By the National Machinery Industry standard JB/T9014.9-1999, the bevel plane was raised at a constant speed until the slide block began to slide. During the test, high-speed cameras were used to record the slide block[27], and the PFV4 image processing software was used to extract the angle value associated with the lifting of the bevel plane meter at the instant when the slide block moves. Equation (1) was used to determine the static sliding friction coefficient f_s [7].

$$f_s = f/N = G\sin\beta/G\cos\beta = \tan\beta \quad (1)$$

where, f_s is the static sliding friction coefficient; f, N, and G are the friction force, supporting force, and gravity, respectively, N; β is the static sliding friction angle, (°).

2.2.2 Procedure for testing the friction properties between an external contact material and peanut straw

In this section, the static sliding friction coefficient (f_s) and static rolling stability angle (μ_e) between the peanut straw and residual film and between the peanut straw and 40Cr steel plate under different moisture contents and particle sizes were studied. As it is difficult to define the degree of entanglement between the residual film and peanut straw and the degree of damage on the straw surface, an untreated peanut straw with an intact surface was taken as the research subject. Soil screens of different diameters were used to screen the film mixture that had been chopped and pretreated, and the particle size distribution of the comminuted material was between 0-30 mm. Specifically, comminuted materials with length ranges of 2-5 mm, 5-10 mm, and 10-20 mm accounted for the largest proportion, accounting for 45.37%, 33.60%, and 14.34%, respectively. Therefore, the three particle-size distribution ranges of the peanut straw were taken as one of the influencing factors in the test on the friction characteristics.

During the collection of the peanut straw samples, plants with good verticality, small change in diameter, few branches, no pests, and no damage or fractures were selected. The moisture content in the peanut straw was adjusted following the standards GB/T1928-2009 and GB/T1931-2009. The selected complete straw was placed on a tray in electric drum bellows. The temperature was adjusted to (103±2)°C, and the drying time was 8 h. After drying, the samples with appropriate weights were selected and weighed using an electronic balance to record the weight value. After 2 h, the samples were placed in the bellows again to dry for 8 h under the same conditions and weighed again. The changes in the weight values of the two samples were compared. If the relative change did not exceed 0.5%, the sample was considered dry. The absolutely dry sample was thoroughly soaked with clean water[28], and the soaked sample was cut into different particle sizes (2-5 mm, 5-10 mm, and 10-20 mm) using pruning pliers and then placed in the bellows at a temperature of (45±2)°C, for the actual moisture content in the peanut straw film mixture when chopped and pre-treated. The moisture contents in the samples were adjusted to 20.0%, 30.0%, and 40.0%. When the above peanut stalks with the same appearance were adjusted to exhibit different moisture contents, a large number of samples were used to ensure that the specific moisture content could be adjusted. Moreover, when the same batch of stalks was soaked and the moisture content was measured, a part of the samples was taken out as the products to be tested, and the rest were placed in sealed bags and stored in a cool place without any effect from wind at room temperature. When the product to be tested reached the target moisture content, the sealed sample was used to conduct the test immediately to ensure the consistency of the sample in terms of the sampling location, moisture content, and particle size. The test site was a closed laboratory without ventilation or direct sunlight, to control the adverse effects of unrelated variables, such as the temperature, humidity, and time, on the test to the maximum extent, and reduce the test error as much as possible. Moreover, the sampling after soaking was conducive to the preparation of peanut straw samples with various particle sizes. This helped avoid the phenomenon of straw breakage and splitting caused by excessive drying of the sample during the pruning process. During the preparation of the peanut straw sample, several peanut stalks with good verticality were selected for the adhesion, with the width and length being greater than those of the sample. The surface was relatively flat, and the sliding direction of the sample to be measured was perpendicular to its length. To ensure the controllability of the factors influencing the test, when sampling

peanut straw samples in groups, only a small amount of glue was added to the contact position of the straw, so that no excess glue would overflow to the exposed position outside the sample on the premise of ensuring a firm bond. Moreover, the contact position of the straw was inside the group of samples, and no glue appeared in the contact line or contact surface between the sample and external materials during the test, thus avoiding any change in the test result due to the presence of glue.

The working surface of the bevel meter was covered with an undamaged film, a 40Cr steel plate, and a peanut straw sample with a flat, pressed surface for the static sliding friction test involving peanut straw and external contact materials. Three samples with the same length and adjusted water content were bonded and formed. They were used as a group of peanut stalks and placed at fixed positions on different materials. The length direction of the sample to be measured was perpendicular to the axis direction of the peanut straw on the sample, as shown in Figure 3a. The test was conducted following the JB/T9014.9-1999 National Machinery Industry Standard. The bevel meter was lifted slowly and at a constant speed until the sample to be measured fretted. The static sliding friction coefficient f_s between them was calculated according to Equation (2).

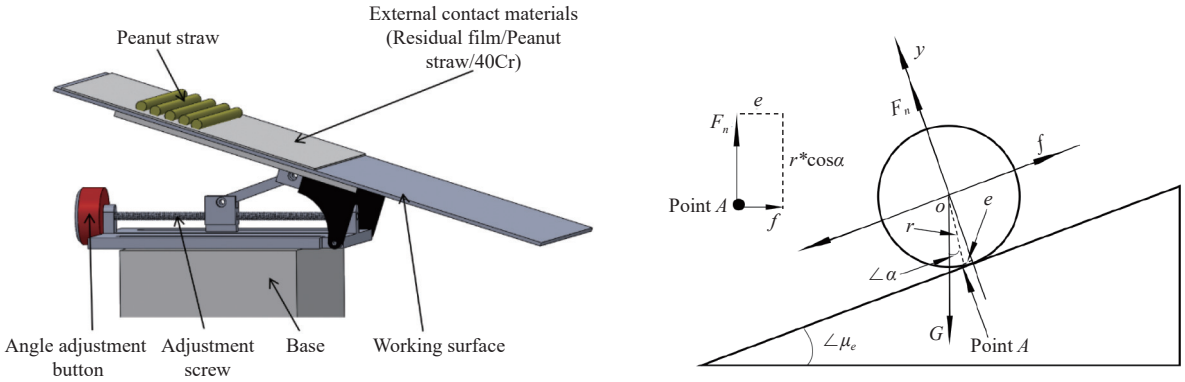

Note: Point A represents the contact point between the straw and the test platform; O, x, and y respectively represent the origin of the coordinates, the x-axis and the y-axis; f, F_n, and G represent friction, support, and gravity, respectively; e and r represent the distance from point A to the origin O and the vertical distance from point A to the y-axis, respectively; $\angle\alpha$ represents the angle between r and the vertical direction; $\angle\mu_e$ represents the angle between the test platform and horizontal plane.

Figure 3 Friction test diagram and friction mechanics analysis diagram

A single peanut straw with a good roundness was placed on the surface of various materials. The position was fixed, and the axis was parallel to the long side of the bevel meter, to measure the straw-material static rolling stability angle under various conditions. The test was conducted in accordance with the National Machinery Industry Standard JB/T9014.9-1999. The bevel meter was lifted slowly and evenly until the sample to be measured began to slide, at which time the angle between the bevel meter and the horizontal plane was analyzed and recorded. As shown in Figure 3b, the single static peanut straw placed on the inclined instrument surface was made to roll. If the external contact surface was deformed, the stress balance and couple balance states of the peanut straw at the action point A can be expressed as follows:

$$\begin{cases} F_n = G \cdot \cos\mu_e \\ f = G \cdot \sin\mu_e \\ F_n \cdot e = f \cdot r \cdot \cos\alpha \end{cases} \tag{2}$$

where, F_n, G, and f are respectively the supporting force, gravity, and friction force, N; e is the vertical distance from the active point A to the y-axis, mm; α is the angle between OA and y-axis, (°); μ_e is the static rolling stability angle, (°).

When the working surface inclination μ_e of the bevel meter gradually increases, the peanut straw breaks the static equilibrium state and begins to roll, and the rolling conditions are as follows:

$$F_n \cdot e \le f \cdot r \cdot \cos\alpha \longrightarrow \tan\mu_e \cdot \cos\alpha \tag{3}$$

where, e/r is the rolling friction coefficient. The rolling friction coefficient is correlated with the static rolling stability angle μ_e, and it was lower than the sliding friction coefficient when compared with Equation (2)[29], which is one of the key conditions for the peanut straw to overcome the rolling resistance. In addition, the sample shape, moisture content, and external contact materials affect μ_e[30].

To determine the frictional properties between the external contact material and the peanut straw, the moisture content a (20%, 30%, and 40%), external contact material b (residual film, 40Cr steel plate, and peanut straw), and material particle size c (2-5 mm, 5-10 mm, and 10-20 mm) were used as the factors influencing the test. F_s (y_1) and μ_e (y_2) were used as the test evaluation indices to conduct three-factor, three-level orthogonal experiments. Table 1 lists the test factors and level codes.

Table 1 Test factors and level codes

Horizontal coded value	Moisture content a	External contact material b	Material particle size c
−1	20%	Peanut straw	2-5 mm
0	30%	40Cr	5-10 mm
1	40%	Residual film	10-20 mm

Based on the levels and test criteria specified in Table 1, the BBD module in the Design Expert was used to conduct orthogonal tests, in which f_s and μ_e measurement tests were conducted in 17 groups, each group of tests was performed thrice, and the arithmetic average was calculated.

3 Analysis of test results

3.1 Examination of the frictional properties between the residual film and the material in contact with it

In the test, a white mulch film that meets the national standard GB13735-2017 and the agronomic requirements of peanut mulch planting in North China was selected as the test material with a

Table 2 Test plan and results

No.	a	b	c	y_1	y_2/(°)
1	−1	−1	0	0.480	5.55
2	1	−1	0	0.505	8.55
3	−1	1	0	0.568	8.85
4	1	1	0	0.669	14.92
5	−1	0	−1	0.529	9.84
6	1	0	−1	0.507	8.70
7	−1	0	1	0.505	6.83
8	1	0	1	0.565	13.98
9	0	−1	−1	0.532	8.83
10	0	1	−1	0.552	8.33
11	0	−1	1	0.459	7.00
12	0	1	1	0.601	11.33
13	0	0	0	0.435	4.43
14	0	0	0	0.445	5.21
15	0	0	0	0.434	4.37
16	0	0	0	0.441	4.85
17	0	0	0	0.437	4.49

thickness of 0.01 mm[31]. Based on the friction test results (Table 2), the static sliding friction coefficient f_s and dynamic sliding friction coefficient f_k between the residual films were in the ranges of 0.33-0.38 and 0.32-0.36, respectively; the lowest and highest inter-film f_s values were in the ranges of 0.331±0.012 and 0.378±0.026, respectively; and the average f_s was 0.360±0.010. The lowest and highest intermembrane (f_k) values were in the ranges of 0.322±0.023 and 0.361±0.03, respectively, and the average f_k was 0.340±0.050. The static sliding friction coefficient (f_s) between the film and the 40Cr steel plate was in the range of 0.37-0.39, the minimum and maximum (f_s) values between them were 0.370±0.015 and 0.386±0.042, respectively, and the average f_s was 0.380±0.001.

OriginPro, which is a data processing program, was used to process the test data and produce a normally distributed *Q-Q* curve. Figures 4a and 4b show that the expected normal values of f_s and f_k between the residual films are within the 95% confidence interval and distributed on both sides of the reference line $y=x$, respectively. This suggests that f_s and f_k between the films were normally distributed. Some of the f_s data about the film-40Cr steel, as shown in Figure 4c, coincided with the lower limit of the 95% confidence interval, though most of the measurement results were distributed on both sides of the reference line $y=x$ and in the 95% confidence interval. This indicates that the normal distribution characteristics of the f_s data for the film-40Cr steel were slightly different from the first two.

3.2 Results of variance regression analysis and model construction of orthogonal experiment

The p-values of the interaction items a^2, b^2, and c^2 as well as the single-factor b were all less than 0.01, as listed in Table 3, for the static sliding friction coefficient y_1 of the test response index. This indicates that these factors are important in influencing the y_1 value. Both the interactive item bc and the single-factor item a had p-values between 0.01 and 0.05, indicating that they were significant factors influencing y_1. All the interaction items (ab and ac) and the single-factor item c had p-values greater than 0.05, indicating that they were not significant factors influencing y_1. The degree of influence of highly significant and significant factors and their interaction items on the response index y_1 can be ranked as $b>b^2>a^2>c^2>bc>a$.

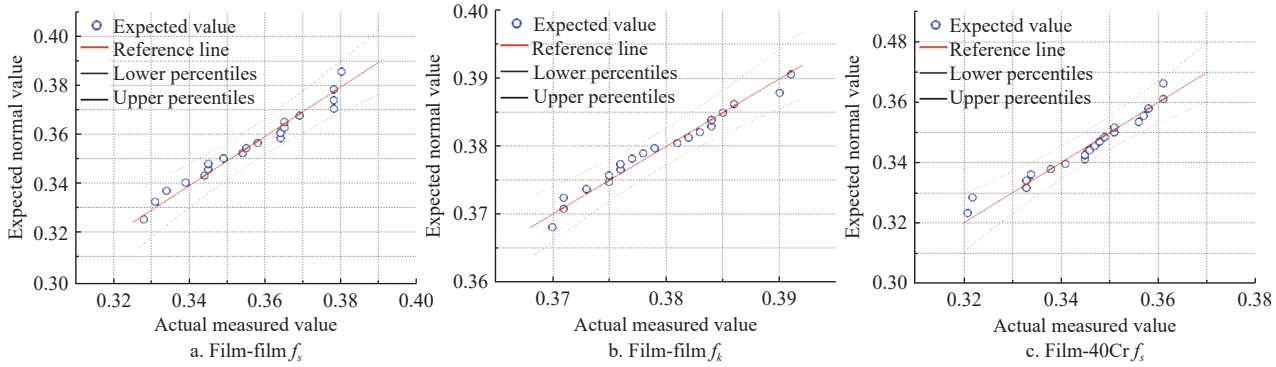

Figure 4 Normally distributed *Q-Q* diagrams

For the static rolling stability angle y_2, the p-values of the single-factor items a and b, and the interactive items ac, a^2, b^2, and c^2, were all less than 0.01, indicating that they were extremely significant factors influencing y_2. The p-value of bc was between 0.01 and 0.05, and it was a significant factor influencing y_2. Both the interaction item ab and the single component c had p-values greater than 0.05, indicating that they were not significant factors influencing y_2. The degree of influence of the highly significant and significant factors and their interaction items on the response index y_2 could be ranked as $a^2>a>b>c^2>ac>b^2>bc$.

According to the regression and variance analysis in Table 3, the second-order response model between y_1, y_2, and the influencing factors established in this study is extremely significant (p=0.0003<0.01), and both have the same p-value of 0.0003. Meanwhile, the determination coefficient of y_1 model is R^2=0.9654, the correction determination coefficient R^2_{adj}=0.9210, and the coefficient of variation CV=3.70%. The determination coefficient R^2=0.9630, correction determination coefficient R^2_{adj}=0.9155, and variation coefficient CV=11.65% of the y_2 model are all within the allowable range, indicating that there is a high correlation between the three test factors and the two response indicators y_1 and y_2, and the constructed mathematical model has high explanatory power and is stable. This model can be used to predict the f_s and μ_e between peanut stems and different materials with different moisture content.

The following is the construction of the second-order response model between the test response indices y_1 and y_2 and test influencing factors a, b, and c:

$$y_1 = 0.4384 + 0.0205*a + 0.051\,75*b + 0.001\,25*c + 0.019*ab + 0.0205*ac + 0.0305*bc + 0.0538*a^2 + 0.0633*b^2 + 0.0343*c^2;$$

$$y_2 = 4.67 + 1.885*a + 1.6875*b + 0.43*c + 0.7675*ab + 2.0725*ac + 1.2075*bc + 2.881\,25*a^2 + 1.916\,25*b^2 + 2.286\,25*c^2. \quad (4)$$

In summary, both the moisture content a and the external contact material b significantly influenced the friction characteristics f_s and f_k. In particular, the external contact material b had the greatest impact on these characteristics, whereas the straw particle size c had little impact on the friction characteristics.

Table 3 Variance regression analysis of experimental data

Source	df	y_1				y_2			
		SS	MS	F-value	p-value	SS	MS	F-value	p-value
Model	9	0.0693	0.0077	21.71	0.0003**	158.66	17.63	20.27	0.0003**
a	1	0.0034	0.0034	9.47	0.0179*	28.43	28.43	32.68	0.0007**
b	1	0.0214	0.0214	60.37	0.0001**	22.78	22.78	26.19	0.0014**
c	1	0.0000	0.0000	0.0352	0.8565−	1.48	1.48	1.70	0.2335−
ab	1	0.0014	0.0014	4.07	0.0835−	2.36	2.36	2.71	0.1438−
ac	1	0.0017	0.0017	4.74	0.0660−	17.18	17.18	19.75	0.0030**
bc	1	0.0037	0.0037	10.49	0.0143*	5.83	5.83	6.70	0.0360*
a^2	1	0.0122	0.0122	34.34	0.0006**	34.95	34.95	40.18	0.0004**
b^2	1	0.0169	0.0169	47.54	0.0002**	15.46	15.46	17.77	0.0040**
c^2	1	0.0050	0.0050	13.96	0.0073**	22.01	22.01	25.30	0.0015**
Residual	7	0.0025	0.0004			6.09	0.8698		
Lack of fit	3	0.0024	0.0008	38.48	0.0021	5.58	1.96	14.77	0.0125
Pure error	4	0.0001	0.0000			0.5040	0.1260		
Cor total	16	0.0718				164.75			
		R^2=0.9654, R^2_{adj}=0.9210, $C.V$=3.70%				R^2=0.9630, R^2_{adj}=0.9155, $C.V$=11.65%			

Note: SS is the sum of squares; MS is the mean square. ** indicates extremely significant influencing factors (p<0.01); * indicates significant influencing factors (0.01<p<0.05); − indicates nonsignificant influencing factors (p>0.05).

3.3 Analysis of the influence of a single factor on the friction characteristics between peanut straw and external contact material

3.3.1 Examination of the impact of a single factor on the static sliding friction coefficient

The model curve A in Figure 5a first exhibits a downtrend and then climbs with the increase in the level of the test factor a. y_1 exhibited a downtrend as the influence factor a increased from −1 to 0. This implies that as the moisture content increased, the static sliding friction coefficient between the peanut straw and external contact material gradually decreased, though the trend was not very noticeable. This is because a small amount of hydrophobic fluff remained after the aging of the straw surface. With the increase in the moisture content, the hydrophobic action of villi will make the contact area between the two smaller, and the value of moisture content has not reached the deposit of liquid film between the contact surface of the two[32]. Therefore, the reduction in the contact area leads to a decrease in the static sliding friction coefficient. With further increase in the moisture content, the surface humidity of the straw increased, and a liquid film was formed between the straw and the external contact material due to adsorption or deposition, thus forming a meniscus force around the contact surface[33], resulting in an additional friction force. This increased the static sliding friction coefficient. Therefore, when the level of factor A changed from 0 to 1, y_1 showed an uptrend. Hou[34] also found that when the moisture content is less than 20%-30% on the contact plane between maize stalk and wood, the friction coefficient between the maize stalk and wood decreases with the increase in the moisture content. Moreover, Yang et al.[35] found that when the moisture content of broom corn millet is lower than 15.5%, the sliding friction coefficient first changes gently and then increases rapidly after exceeding 15.5%. Wang et al.[36] described the same phenomenon when studying the sliding friction coefficient between the rice stalk and steel roller caused by the moisture content in the rice stalk.

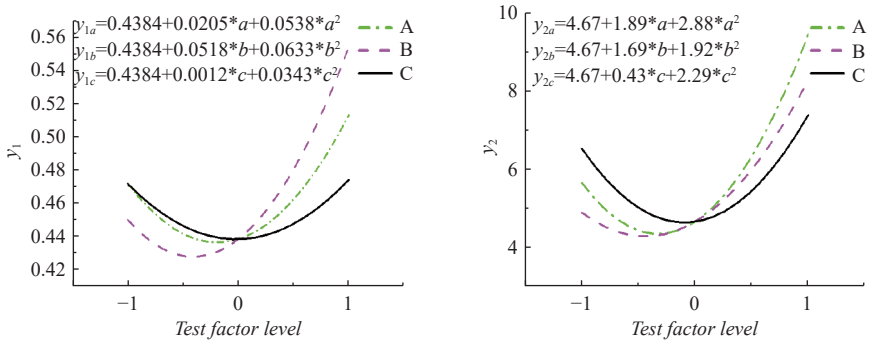

a. Static sliding friction coefficient b. Static rolling stability angle

Figure 5 Effects of single factor on static sliding friction coefficient and static rolling stability angle

The model curve B in Figure 5a first exhibits a downtrend and then climbs with the increase in the level of the test factor b. When the level of the test factor b=1, that is, in the presence of peanut straw and residual film, the static sliding friction coefficient increased to its maximum value of 0.553. At this time, the contact area between the two was greater than the contact area between the straws and between the straw and the 40Cr steel plate, resulting in a higher static sliding friction coefficient. For the other two types of external contact materials, the f_s value between the straws was greater than that between the straw and 40Cr steel plate. This is because the peanut straw sample in the test was not a regular long straight cylinder under ideal conditions. Therefore, when it contacted the 40Cr steel plate, the contact was not a regular line contact nor a surface contact but a multi-point or multi-line contact. Hence, the f_s value when the two contacted was low. When the straws were in contact with each other, because the roughness of the straw surface was greater than that of the 40Cr steel plate, f_s was greater than that when the straw was in contact with the 40Cr steel plate. Baryeh et al.[37] investigated the friction coefficient between Bambara peanuts and various exterior contact materials. Due to the varying roughness on the contact surface, the contact between the peanuts and different surfaces showed different frictional characteristics: the friction coefficients between the peanuts and plywood, iron plate, and aluminum plate gradually decreased.

The model curve C in Figure 5a shows a tendency of first decreasing and then increasing with the increase in the level of the test factor c, though the overall change value is within the range of 0.034 00±0.000 45, and the change rate is less than 7.5%. This also

indicated that the test factor *c* had little influence on the frictional characteristics of the peanut straw. The reason for this change was that with the change in the straw particle size, the influence of the surface shape on its frictional characteristics became more pronounced. The smaller the particles, the more similar the diameter and length of the straw. The originally irregular cylinder became a straight one due to the reduction in the length. Therefore, the multi-line contact between the contact surfaces became a surface contact, leading to a high static sliding friction coefficient of the test factor *c* at the −1 level. When the level of the test factor *c* was 1, due to the larger grain size of the straw, its curvature became the main factor affecting the friction characteristics, and a multi-point or multi-line contact was formed between the contact surfaces, rather than an ideal line contact, resulting in a higher static sliding friction coefficient at this level. Huo et al.[38] studied the physical properties of crop straw raw materials and found that the friction and flow characteristics of the raw materials were closely related to the particle size of the raw materials. Wang et al.[39] also found a similar trend when studying the influence of the particle size on the Carr index of pulverized coal. The comprehensive flow index of the pulverized coal first decreased and then increased with the increase in the force within the test range, and the flow index of the materials was related to their friction characteristics.

3.3.2 Examination of the impact of a single factor on static rolling stability angle

The model curve *A* in Figure 5b represents the relationship between the moisture content in the peanut straw and the static rolling stability angle y_2 when the levels of the test factors *b* and *c* were 0. With the change in the level of the test factor *a* from −1 to 1, the model curve *A* showed a trend of first decreasing and then increasing; that is, with increasing moisture content, the static rolling stability angle of the straw showed a tendency of decreasing initially and then increasing. The maximum static friction force that must be overcome by straw rolling progressively dropped during the y_2 reduction stage or as the moisture content increased. This reduced the static rolling stability angle between the straw and the external contact material. In the y_2 increasing stage, that is, with further increase in the moisture content, capillary condensation or a thin water film was formed between the contact surfaces of the straw, generating adhesion[33] and resulting in a greater friction force. Therefore, a greater tilt angle was required for the peanut straw, until it began to roll when the gravity force along the inclined instrument surface overcame the friction force.

As shown in Figure 5b, with the increase in the test factor *b* from −1 to 0, the trend in model curve *B* remains unchanged. In comparison, with the increase in the test factor *b* from 0 to 1, the model curve showed an increasing trend, and the rolling angle gradually increased from 4.900° to 8.274°. That is, the straw and straw with 40Cr steel plate had very small static rolling stability angles. The straw and residual film had a reasonably large static rolling stability angle. Due to the texture characteristics of the straw surface, there was a multi-point contact between the straws. The stable angle for static rolling between the stalks may be small when the inclination angle is small because the component force of the straw gravity along the inclined plane overcomes the friction force and the straw rolls. During the friction between the straw and the 40Cr steel plate, the static rolling stability angle decreases due to the influence of the surface structure and smoothness of the straw. Due to the high degree of softness of the residual film, it can easily deform after being stressed, forming a deformation resistance[40], which affects its rolling stability and prevents the straw from rolling. This results in the formation of a significant static rolling stability angle between the straw and the residual film.

In Figure 5b, when the level of the test factor *c* changes from −1 to 1, the model curve *C* presents a trend of first decreasing from 6.526° to 4.850°, and then increasing to 7.386°, and the overall change trend is not evident. This also corresponds to the result of the orthogonal test, where the *p*-value is greater than 0.05, which is not a significant factor influencing the response index y_2. With the increase in the straw grain size, the curve first shows a downtrend. This is because compared with small particles, larger particles have a more uniform surface roughness. Therefore, the surface of larger grain-size straws shows a smaller static rolling stability angle. Zhang et al.[21] also described this change when studying the static rolling stability angle of fruits with different grain sizes. However, with a further increase in the particle size, the y_2 value showed an increasing trend. This is because when the straw is too long, the bending degree in the length direction will be more evident, resulting in greater resistance during rolling. This increases the static rolling stability angle of longer straws.

3.4 Examination of test elements that interact to affect the friction properties of peanut straw and the materials it comes into contact with externally

As listed in Table 3, the interaction term *bc* significantly influences the values of y_1 and y_2, and *ac* has a significant impact on y_2. While ignoring the other nonsignificant interaction terms, only the effects of the interaction term *bc* on y_1 and y_2 and the influence of *ac* on y_2 were analyzed.

3.4.1 Examination of the impact of interaction factors on the static sliding friction coefficient

As shown in Figure 6, when the influence factor *b* (external contact material) is peanut stalk, i.e., the level of the factor is −1 and remains unchanged, the response index y_1 (static sliding friction coefficient) shows a downtrend and then an uptrend as the influence factor *c* (particle size) varies from a range of 2-5 mm to a range of 10-20 mm. This law is similar to that of the effect of the single factor *c* on y_1. However, under the interaction between influencing factors *b* and *c*, the downtrend is slightly more prominent than the uptrend. This law and the effect of the single factor *c* on y_1 are different. This difference is likely due to the combined effect of the two factors *b* and *c* on the response index y_1.

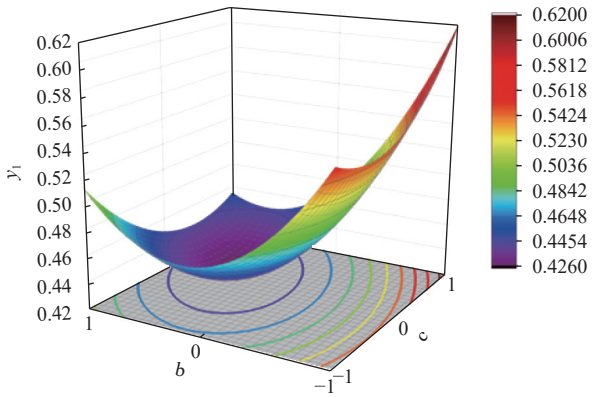

Figure 6 Change trend of the interaction term *bc* influencing y_1

When the influence factor *b* (external contact material) is the residual film, i.e., the factor level is 1 and remains unchanged, and as the influence factor *c* (particle size) varies from a range of 2-5 mm to a range of 5-10 mm, the response index y_1 shows a declining trend and then a rising trend. The difference is that the downtrend is slightly less pronounced than the uptrend. The effect

of the single factor c on y_1 is close to this law.

As the influence factor c (particle size) takes values in the range of 2-5 mm, i.e., the factor level is −1 and remains unchanged, and as the influence factor b (external contact material) is changed from peanut stalks to 40Cr steel plate and residual film, the response index y_1 (static sliding friction coefficient) tends to decrease first and then increase, with the rate of decrease being lower than the rate of increase. This law is similar to the effect of the single factor b on the response index y_1.

When the influence factor c (particle size) takes values in the range of 10-20 mm, i.e., the factor level is 1 and remains unchanged, the effect of b on the response index y_1 is similar.

When the influence factor c (particle size) takes values in the range of 10-20 mm, i.e., the factor level is 1 and remains unchanged, and as the influence factor b (external contact material) is changed from peanut stalks to 40Cr steel plate, the response index y_1 remains unchanged at first and then exhibits an uptrend. In particular, when the external contact material is changed from 40Cr steel plate to the residual film, the response index y_1 remains unchanged at first and then exhibits an uptrend. When the external contact material is changed from the 40Cr steel plate to the residual film, y_1 increases significantly; this law is the same as that of the effect of the single factor b on y_1.

In addition, in the process of the influencing factor b, i.e., when the outer contact material is changed from peanut stalks to 40Cr steel plate and residual film, and in the process of the influencing factor c, i.e., when the particle size increases from a range of 2-5 mm to a range of 10-20 mm, y_1 shows a decreasing and then increasing trend. Moreover, the static sliding friction coefficient of the peanut stalks, y_1, reaches a maximum value of 0.618 when the influencing factors b and c reach their highest levels.

3.4.2 Examination of the impact of interaction terms on static rolling stability angle

As shown in Figure 7a, when the influencing factor a (moisture content) is 20%, i.e., the factor level is 1 and remains unchanged, the response index y_2 (static rolling stability angle) tends to decrease and then increase in the process of varying the influencing factor c (particle size) from a range of 2-5 mm to a range of 10-20 mm. This law is the same as that of the effect of the single factor c on y_2, with the rate of decrease being greater than the rate of increase. When the influence factor a (moisture content) is 40%, that is, the factor level is 1 and remains unchanged, as the influence factor c (particle size) increases from a range of 2-5 mm to a range of 10-20 mm, the response indicator y_2 (static rolling angle of stability) first remains unchanged and then exhibits a rising trend. This law is slightly different from the effect of the single factor c on y_2.

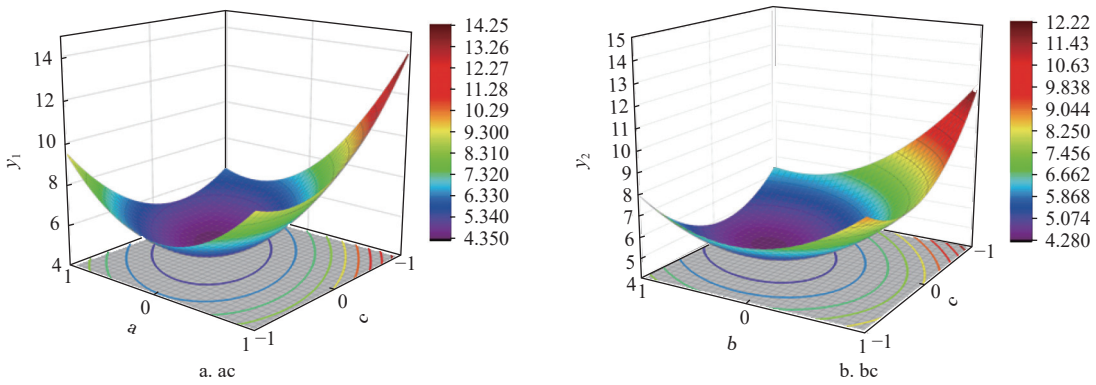

a. ac b. bc

Figure 7 Interaction term ac affects the change trend of y_1 and interaction term bc affects the change trend of y_2

When the value of the influence factor c (particle size) is in the range of 2-5 mm, i.e., the factor level is −1 and remains unchanged, as the influencing factor a (moisture content) varies from 20% to 40%, the response index y_2 tends to decrease first and then increase. This law is similar to the effect of the single factor a on y_2, while the rate of decrease and rate of increase of y_2 tend to be the same.

When the influencing factor c (particle size) is in the range of 10-20 mm, i.e., the factor level is 1 and remains unchanged, as the influence factor a (water content) varies from 20% to 40%, the response index y_2 remains unchanged and then tends to increase, with the rate of increase being relatively high. At the same time, as the influence factor a (water content) increases from 20% to 40% and the influence factor c increases from 2-5 mm to 10-20 mm, y_2 remains unchanged and then increases.

As the influence factor a (water content) increases from 20% to 40% and the influence factor c increases from 2-5 mm to 10-20 mm, y_2 remains unchanged and then increases.

As the influencing factor a (water content) increases from 20% to 40% and the influencing factor c increases from 2-5 mm to 10-20 mm, y_2 tends to decrease and then increase. As the moisture content a reaches the highest value of 40% and the particle size c reaches the highest value of 10-20 mm, the static rolling angle of stability y_2 reaches its maximum value of 14.03°.

The influencing factor a (water content) has a greater influence on y_2 than the influencing factor c (particle size).

As shown in Figure 7b, when the influencing factor b (external contact material) takes peanut stalk and residual film, i.e., the factor levels are −1 and 1, respectively, and as the influencing factor c (particle size) varies from 2-5 mm to 10-20 mm, the response index y_2 tends to decrease first and then increase. This law is similar to the effect of the single factor c on y_2, with the rate of decrease of y_2 being lower than the rate of increase. When the influence factor c takes values in the range of 2-5 mm, that is, the factor level is −1 and remains unchanged, and as the influence factor b sequentially changes from peanut stalks to the residual film, the response index y_2 tends to first decline and then increase. This law and the effect of the single factor b on y_2 are the same, with the rate of increase being greater than the rate of decrease. As the influence factor c takes values in the range of 10-20 mm, that is, the factor level is 1 and remains unchanged, and as the influence factor b sequentially changes from peanut stalks to the residual film, the response index y_2 presents a rising trend. This law and the effect of the single factor b on y_2 are the same, with the rate of increase being greater than the influence factor c alone when the role of the rising speed. That is, the influence of factor b on y_2 is greater than that of factor c. In addition, as the influencing factor b changes from peanut stalks to

residual film and the influencing factor c changes from a range of 2-5 mm to a range of 10-20 mm, y_2 tends to decrease and then increase. When the external contact material is the residual film, and the particle size c reaches the highest value of 10-20 mm, the static rolling stability angle y_2 reaches a maximum value of 12.016°.

4 Conclusions

In this study, the friction coefficient between residual films and between the residual film and 40Cr steel plate was studied using a static and dynamic friction coefficient instrument. Moreover, a mathematical model of the friction characteristics between peanut stems and different materials with different water contents and different stalk-crushing grain sizes was established based on the bevel meter and response surface method, and the influence laws of the above three factors on the friction characteristics were studied. The established model could effectively reflect and predict the influence laws of the above three factors on the friction characteristics of peanut stems. The specific conclusions are as follows:

1) The mean value of the static sliding friction coefficient f_s between the residual film and the residual film was in the range of 0.33-0.38, the mean value of the dynamic sliding friction coefficient f_k was in the range of 0.32-0.36, and the mean value of the static sliding friction coefficient f_s between the residual film and 40Cr steel plate was in the range of 0.37-0.39, all of which conform to the normal distribution characteristics. The measured data were within the upper and lower limits of the 95% confidence intervals.

2) Based on the test data and the level setting of each factor, the Box-Behnken module was used to construct three factors: second-order response models between the moisture content, external contact material, particle size, static sliding friction coefficient, and static rolling stability angle of the response index. The p-values of the two models showed that the simulation data of the mathematical model obtained were highly consistent with the real data measured in the test. Moreover, the coefficient of determination R^2, the modified coefficient of determination R^2_{adj}, and the coefficient of variation CV were all within the effective range. This indicated that the above three influencing factors, the static sliding friction coefficient of the dependent variable, and the static rolling stability angle exhibited the characteristics of high fit, high resolution, and good predictability.

3) The orthogonal test results showed that the two response indicators (static sliding friction coefficient (y_1) and static rolling stability angle (y_2)) with the influence of factors a and b, namely, the moisture content and particle size of the peanut stalks, were first negatively correlated and then positively correlated. When the stalk moisture content was at its maximum value of 40% and the particle size was at its maximum value in the range of 10-20 mm, y_2 reached its maximum value, 14.038°. When the outer contact material was changed from peanut stalks to 40Cr steel plate and residual film in turn, the two response indicators first exhibited a declining trend and then a rising trend in the outer contact material for the residual film and particle size to reach the maximum value, and y_1 also reached the maximum value of 0.618.

4) To study the friction characteristics of peanut straw, residual film, and other external contact materials, the friction parameters were systematically tested and analyzed in this study. These tribological data not only provide a solid theoretical basis for the design and optimization of peanut straw crushing equipment, but also lay a scientific foundation for the research, development, and manufacturing of straw and residue film separation equipment. Through an accurate understanding of friction parameters, our findings can help improve the work efficiency and stability of related equipment, promote the high-quality development of agricultural mechanization, and provide important technical support for the further innovation of modern agricultural technology and equipment.

Acknowledgements

This study was supported by the National Nature Foundation Project (Grant No. 52175238), the Key Research and Development Plan Project of Xinjiang Autonomous Region (Grant No. 2022B02022-1), the integrated pilot project of agricultural machinery Research and Development, Manufacturing and Application in Shandong Province (Grant No. NJYTHSD-202321), and the Ministry of Industry and Information Technology residual film recycling machine project (23128). The data of this study will be made available upon request.

[References]

[1] Li H D, Li W J, Kang T, Zhang L M, Chen J S, Zhang Y Y, et al. Effects of different harvesting periods on yield and constituent factors of peanut under open-field cultivation conditions. Journal of Peanut Science, 2021; 50(3): 75–79.

[2] Zhao Y, Chen X G, Wen H J, Zheng X, Niu Q, Kang J M. Research status and prospect of farmland residual film pollution control technology. Transactions of the CSAM, 2017; 48(6): 1–14.

[3] Liu X L, Zhao W Y, Zhang H, Wang G P, Sun W, Dai F, et al. Design and experiment of an upper-side-discharge straw-returning and bundle self-unloading integrated maize residual film recycling machine. Int J Agric & Biol Eng, 2023; 16(5): 61–70.

[4] Tang Z, Liang Y Q, Wang M L, Zhang H, Wang X Z. Effect of mechanical properties of rice stem and its fiber on the strength of straw rope. Industrial Crops and Products, 2022; 180: 114729.

[5] Gu F W, Zhao Y Q, Wu F, Hu Z C, Shi L L. Simulation analysis and experimental validation of conveying device in uniform rrushed straw throwing and seed-sowing Machines using CFD-DEM coupled approach. Computers and Electronics in Agriculture, 2022; 193: 106720.

[6] Larsson S H. Kinematic wall friction properties of reed canary grass powder at high and low normal stresses. Powder Technology, 2010; 198(1): 108–113.

[7] Subramanian S, Viswanathan R. Bulk density and friction coefficients of selected minor millet grains and flours. Journal of Food Engineering, 2007; 81(1): 118–126.

[8] Kruggel-Emden H, Simsek E, Rickelt S, Wirtz S, Scherer V. Review and extension of normal force models for the Discrete Element Method. Powder Technology, 2007; 171(3): 157–173.

[9] Cleary P W. Industrial particle flow modelling using discrete element method. Engineering Computations, 2009; 26(6): 698–743.

[10] Shafaei S M, Nourmohamadi-Moghadami A, Kamgar S. Experimental analysis and modeling of frictional behavior of lavender flowers (*Lavandula stoechas* L.). Journal of Applied Research on Medicinal and Aromatic Plants, 2017; 4: 5–11.

[11] Grift T E, Kweon G, Hofstee J W, Piron E, Villette S. Dynamic friction coefficient measurement of granular fertiliser particles. Biosystems Engineering, 2006; 95(4): 507–515.

[12] Kweon G, Grift T E, Miclet D. A spinning-tube device for dynamic friction coefficient measurement of granular fertiliser particles. Biosystems Engineering, 2007; 97(2): 145–152.

[13] Shafaei S M, Nourmohamadi-Moghadami A, Kamgar S. Analytical study of friction coefficients of pomegranate seed as essential parameters in design of post-harvest equipment. Information Processing in Agriculture, 2016; 3(3): 133–145.

[14] Zhao Z, Huang H D, Yin J J, Yang S X. Dynamic analysis and reliability design of round baler feeding device for rice straw harvest. Biosystems Engineering, 2018; 174: 10–19.

[15] Fang X, Chen H T, Huang Z H, Li L X. Sliding friction characteristic of different moisture content of soybean stalk with different materials.

Soybean Science, 2012; 31(5): 838–841.
[16] Sui M L. 2005. Logistics analysis and computer simulation of the homogenized filling area of straw baling feed machine. Master dissertation. Baoding: Hebei Agricultural University, 2005; 52p. (in Chinese) doi: 10.7666/d.y740280.
[17] Shinners K J, Koegel R G, Lehman L L. Friction coeficient of Alfalfa. Transactions of the ASAE, 2013; 34(1): 33–37.
[18] Li Y J, He F, Bo X Y, Yi W M. Sliding friction coefficient of particle and powder mixture along inclined slide. Journal of Shandong University of Technology (Natural Science Edition), 2003; 4: 10–12. (in Chinese)
[19] Adapa P, Tabil L, Schoenau G. Physical and frictional properties of non-treated and steam exploded barley, canola, oat and wheat straw grinds. Powder Technology, 2010; 201(3): 230–241.
[20] Yang Z M, Guo Y M, Cui Q L, Li H B. Test and influence factors analysis of friction characteristics of millet. Transactions of the CSAE, 2016; 32(16): 258–264. (in Chinese)
[21] Zhang Q, Ding W M, Deng L J, Li Y N, Zhao Y P. Experimental study on friction characteristics in real mechanical husking. Transactions of the CSAE, 2013; 29(1): 56–63. (in Chinese)
[22] Lu F Y, Ma X, Tan S Y, Chen L T, Zeng L C, An P. Simulation calibration and experiment om main contact parameters of discrete elements for rice bud seeds. Transactions of the CSAM, 2018; 49(2): 93–99. (in Chinese)
[23] Lu C Y, Zhao C J, Meng Z J, Wang X, Wu G W, Gao N N. Straw friction characteristic based on rotary cutting anti-blocking device with slide plate pressing straw. Transactions of the CSAE, 2016; 32(11): 83–89. (in Chinese)
[24] Liang R Q, Chen X G, Jiang P, Zhang B C, Meng H W, Peng X B, et al. Calibration of the simulation parameters of the particulate materials in film mixed materials. Int J Agric & Biol Eng, 2020; 13(4): 29–36.
[25] Liang R Q, Zhang L P, Jiang P, Jia R, Meng H W, Kan Z, et al. Study on friction characteristics between cotton stalk-residual film-external contact materials. Industrial Crops and Products, 2024; 209: 118022.
[26] Liang R Q, Zhang B C, Chen X G, Meng H W, Wang X Z, Shen C J, et al. Design and test of a multi-edge toothed cutting device for membrane impurity mixed material. Int J Agric & Biol Eng, 2023; 16(2): 73–84.
[27] Cui T, Liu J, Yang L, Zhang D X, Zhang R, Lan W. Experiment and simulation of rolling friction characteristics of corn seed based on high-speed photography. Transactions of the CSAE, 2013; 29(15): 34–41. (in Chinese)
[28] Hirai Y, Inoue E, Mori K, Hashiguchi K. PM - Power and machinery: Investigation of mechanical interaction between a combine harvester reel and crop stalks. Biosystems Engineering, 2002; 83(3): 307–317.
[29] Zhang C, Du W L, Chen Z, Surigalatu. Contact parameter measurement and discrete element simulation calibration of buckwheat rice screening material. Journal of Agricultural Mechanization Research, 2019; 41(1): 46–51. (in Chinese)
[30] Xiao J Z, Lei J L, Li Q, Niu Z H, Yin S H. Research on straw friction characteristics based on small straw round baler. Journal of Agricultural Mechanization Research, 2022; 44(4): 133–140. (in Chinese)
[31] Zhou Z Q. Mulching technology of spring peanut. Agriculture of Henan, 2021; 27: 56–57. (in Chinese)
[32] Shi W S, Liu J L, Su Y Y, Wang B. Effects of water content on tribological properties and oil yield of water gourd. Journal of Agricultural Mechanization Research, 2007; 6: 120–122, 125. (in Chinese)
[33] Liu S S, Zhang Z H, Liu J M. Calculation of meniscus forces in microplane contact separation. Acta Physica Sinica, 2010; 59(10): 6902–6907. (in Chinese)
[34] Hou J. Mechanical properties and physicochemical indexes of corn straw and their correlation. Master dissertation. Harbin: Northeast Agricultural University, 2013; 110p.
[35] Yang Z M, Guo Y M, Cui Q L, Li H B. Experimental study on friction characteristics of broomcorn millet with different moisture content. Journal of Shanxi Agricultural University (Natural Science Edition), 2016; 36(7): 519–523. (in Chinese)
[36] Wang D F, Jiang Z G, Li B Q, Wang G F, Jiang Y Y. Experiment on sliding friction characteristics between rice straw and baler steel-roll. Transactions of the CSAE, 2017; 33(21): 44–51. (in Chinse)
[37] Baryeh E A. Physical properties of bambara groundnuts. Journal of Food Engineering, 2001; 47(4): 321–326.
[38] Huo L L, Tian Y S, Zhao L X, Yao Z L, Hou S L, Meng H B. Research on physical characteristics and testing methods of crop straw raw materials. Renewable Energy Resources, 2011; 29(6): 86–92. (in Chinese)
[39] Wang Y H, Gao B, Song Z P, Chen J. Study on the influence of particle size on Carr index of pulverized coal. In: Proceedings of the 4th Chinese Metal Society Youth Academic Annual Conference. Chinese Society of Metals, 2024; pp.40–43. (in Chinese)
[40] Guo J L. Influence of deformation of stressed body on rolling friction resistance. Gansu Science and Technology, 2006; 8: 146–147. (in Chinese)